



Invariants of Multi-linkoids

Boštjan Gabrovšek  and Neslihan Gügümcü

Abstract. In this paper, we extend the definition of a knotoid to multi-linkoids that consist of a finite number of knot and knotoid components. We study invariants of multi-linkoids, such as the Kauffman bracket polynomial, ordered bracket polynomial, the Kauffman skein module, and the T -invariant in relation with generalized Θ -graphs.

Mathematics Subject Classification. Primary 57K12; Secondary 57M15.

Keywords. Knotoid, multi-linkoid, spatial graph, Kauffman bracket polynomial, Kauffman bracket skein module, theta-curve, theta-graph.

Introduction

Knotoids were defined by Turaev [39] as immersions of the unit interval in surfaces. Knotoids are open-ended knots with two endpoints that can lie anywhere in the surface. In this sense, the theory of knotoids in S^2 generalizes classical knot theory and has a natural connection with the theory of virtual knots [22, 23] through the *virtual closure*. Intrinsic invariants of knotoids, as well as invariants induced from classical and virtual knot invariants have been studied by many researchers. See [3–5, 14–16, 19, 20, 25, 26, 29, 36, 39]. Turaev showed that knotoids in S^2 are in one-to-one correspondence with simple Θ -curves and multi-knotoids in S^2 , immersions of the unit interval and a finite number of circles in S^2 , are in one-to-one correspondence with simple theta-links [39]. Later, knotoids in \mathbb{R}^2 were described as open space curves in $\mathbb{R}^3 \setminus \{\text{two parallel lines}\}$ in [14] or as rail arcs in [24].

Topological structures are also an emerging field in modern chemistry [9] as knots have been identified in DNA [34] and proteins [27, 40]. Research suggests that the existence of knotting increases thermal and kinetic stability of the molecule [35], as well as to have important functional roles [40]. A protein's backbone natively forms an embedded interval in 3-space. Classical studies of protein topology (i.e. determining the knot type) rely on closing this interval by some closure method (closure methods are thoroughly discussed in [28]). Since closures are often ambiguous (in the case when the protein termini are not located close to the minimal convex surface enveloping the

protein), knotoids have been identified as natural candidates to study open-knotted proteins [12, 13, 18].

One can extend the notion of a knotoid by considering several closed and open-ended components. A *multi-linkoid* is a union of a finite number of immersed unit intervals and circles in a closed orientable surface. The main goal of this paper is to generalize the mentioned concepts to multi-linkoids and to introduce invariants for them. We expect that multi-linkoids would suggest a new setting for the topological analysis of several mutually entangled physical systems such as polymer chains or subchains via the invariants we introduce here.

The paper is organized as follows. Section 1 is an overview of the required notions related to multi-linkoids. In Sect. 2 we extend the Kauffman bracket polynomial to multi-linkoids. In addition, we strengthen this invariant to the ordered Kauffman bracket polynomial for multi-linkoids with an ordering on its knotoid components. In Sect. 2.1, we introduce the Kauffman skein module of multi-linkoids and show that the module is freely generated. In Sect. 3, we study multi-linkoids in a geometric setting. We introduce simple generalized Θ -graphs, which are in one-to-one correspondence with multi-linkoids, where we take also into consideration the possibility of an ordering on the components.

In Sect. 4, we utilize the T -invariant for spatial graphs [21] and strengthen it by introducing the colored T -invariant for distinguishing multi-linkoids and ordered multi-linkoids.

1. Preliminaries

We begin with a presentation of fundamental notions we will use throughout the paper.

Definition 1.1. [39] A *knotoid diagram* K in a surface Σ is a generic immersion of the unit interval $[0, 1]$ into Σ . The immersion K is generic in the sense that there are only a finite number of intersections of the image curve that are endowed with under or over information, and are regarded as *crossings* of K . The points $K(0)$ and $K(1)$ are considered to be distinct from each other and from any crossings, and are considered as the *endpoints* of K . The endpoints of K are named as the *tail* and the *head*, respectively. A knotoid diagram is oriented from its tail to its head.

A *multi-knotoid diagram* in Σ is a union of a knotoid diagram with a number of knot diagrams in Σ .

We extend the definition of a multi-knotoid diagram to a *multi-linkoid diagram* that is a union of a finite number of knotoid and knot diagrams. We assume an orientation for each component of a multi-linkoid diagram where knotoid components are oriented from tail to head. See Fig. 1.

As in the case of knotoid diagrams [39], we consider multi-linkoid diagrams up to the equivalence relation generated by Reidemeister moves that take place away from the endpoints.

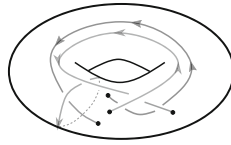


Figure 1. A multi-linkoid diagram with three components on the torus



Figure 2. Reidemeister moves for multi-linkoid diagrams in a surface Σ



Figure 3. The forbidden moves involving the endpoints

Definition 1.2. Two multi-linkoid diagrams in a surface are *equivalent* if and only if they differ by a finite sequence of Reidemeister moves R-0 (surface isotopy), R-I, R-II, and R-III that take place away from the endpoints of the diagrams, shown in the Fig. 2. The endpoints of a multi-linkoid diagram can be displaced by surface isotopy moves without adding/deleting a crossing. In fact, it is forbidden to move an endpoint over or under a strand as illustrated in Fig. 3.

Definition 1.3. A *framed knot* in \mathbb{R}^3 is a knot in \mathbb{R}^3 endowed with a *framing* that is a smooth, everywhere nonzero vector field perpendicular to the knot at each point.

Any knot diagram can be endowed with the *blackboard framing* that is a smooth, everywhere nonzero vector field parallel to the projection plane. The blackboard framing on an oriented knot diagram is determined by the writhe of the knot diagram. Notice that R-0, FR-I, R-II, and R-III moves (presented in Figs. 2 and 4) do not affect the writhe of a knot diagram. A *framed knot* can then be defined as the equivalence class of knot diagrams up to the isotopy relation generated by R-0, FR-I, R-II, and R-III moves. In analogy with this definition, framed knotoids in S^2 are introduced in [29] as follows.



Figure 4. The move FR-I (equivalent to the move $R1'$ in [29].)

Definition 1.4. A *framed knotoid* in S^2 is an equivalence class of knotoid diagrams under the equivalence relation generated by R-0, FR-I, R-II, and R-III moves. A *framed knotoid diagram* is a representation of a framed knotoid in its equivalence class.

This definition can be extended to multi-linkoids directly as follows.

Definition 1.5. A *framed multi-linkoid* in an orientable surface Σ is an equivalence class of multi-linkoid diagrams under the equivalence generated by R-0, FR-I, R-II, and R-III.

We assign to each crossing of an oriented multi-linkoid diagram a sign using the convention $\text{sign} \left(\begin{array}{c} \nearrow \\ \searrow \end{array} \right) = 1$ and $\text{sign} \left(\begin{array}{c} \nwarrow \\ \swarrow \end{array} \right) = -1$.

Definition 1.6. The sum of signs over all crossings of an oriented multi-linkoid diagram of L is called the *writhe*, $w(L)$, of L .

Note that moves R-0, FR-I, R-II, and R-III do not change the writhe, w is thus an invariant of framed oriented multi-linkoids.

We now introduce an ordering on the components of a multi-linkoid diagram.

Definition 1.7. An *ordered multi-linkoid diagram* is a multi-linkoid diagram equipped with an ordering on its open components. An *ordered multi-linkoid* is an equivalence class of ordered multi-linkoid diagrams under the equivalence relation generated by Reidemeister moves given in Fig. 2.

Let L be an ordered multi-linkoid diagram with n knotoid components. The ordering on knotoid components of L induces an ordering of the endpoints. Precisely, for any $i \in \{1, \dots, n\}$ the endpoints of the i^{th} knotoid component of L can be numbered by the pair $(2i - 1, 2i)$ where $2i - 1$ is the number assigned to the tail and $2i$ is the number assigned to the head of the knotoid component. In the sequel, some invariants of multi-linkoid diagrams are constructed with respect to the ordering induced at the endpoints, see Sect. 2 for the ordered Kauffman bracket, Sect. 2.1 for the ordered Kauffman bracket skein module and Sect. 4 for the invariant T_{col} .

Definition 1.8. A *framed ordered multi-linkoid* is an equivalence class of ordered multi-linkoid diagrams considered up to R-0, FR-I, R-II, and R-III moves.

Notice that R-0, FR-I, R-II, and R-III moves do not change the ordering of the components of a multi-linkoid diagram since they take away from the endpoints.

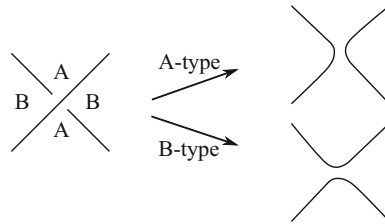


Figure 5. Smoothing types of a crossing

2. Kauffman Bracket Polynomial of Multi-linkoids

In this section, we extend the Kauffman bracket polynomial of knotoids to multi-linkoids in S^2 or \mathbb{R}^2 .

Let L be a multi-linkoid diagram with n crossings. A crossing of L can be smoothed in two ways as follows. First, we consider L to be orientation free. There are exactly four local regions that are incident to each crossing of L . If we rotate the overpassing stand at a crossing counterclockwise for 90 degrees, it passes over two of the four regions incident to the crossing. We call these two regions A regions and the remaining regions B regions (see left hand side of Fig. 5). The A -type smoothing (B -type smoothing) of the crossing removes the crossing and connects the A -regions (B -regions, respectively) as shown in Fig. 5.

By smoothing each crossing of L by applying either an A - or B - type smoothing, we obtain a number of simple closed curves and simple arcs containing the endpoints of L . The disjoint union of the resulting curves forms a state of L that is denoted by σ_i where $i \in \{A, B\}^n$ (an n -ordered tuple of the labels A and B that correspond to smoothing types at crossings of L to obtain σ_i). The collection of closed components of σ_i is denoted by c_{σ_i} and the collection of open components of σ_i is denoted by l_{σ_i} . Each component in c_{σ_i} is evaluated as $-A^2 - A^{-2}$ and each component in l_{σ_i} is associated with the variable λ . We consider $B = A^{-1}$ as for the bracket polynomial of knotoids [39], and we define the bracket polynomial as a Laurent polynomial in the variables A, A^{-1}, λ for L as follows.

Definition 2.1. The *Kauffman bracket polynomial* of L , $\langle L \rangle$ is defined to be the sum

$$\langle L \rangle (A^{\pm 1}, \lambda) = \sum_{\sigma_i} \langle L \mid \sigma_i \rangle (-A^2 - A^{-2})^{\|c_{\sigma_i}\|} \lambda^{\|l_{\sigma_i}\|}, \tag{1}$$

where $\langle L \mid \sigma_i \rangle$ is the product of the labels of the state σ_i , $\|c_{\sigma_i}\|$ is the number of closed components of σ_i and $\|l_{\sigma_i}\|$ is the number of open components of σ_i .

If L is a multi-knotoid diagram, we obtain the bracket polynomial introduced in [39], by the substitution $\lambda = 1$.

Proposition 2.2. *The Kauffman bracket polynomial is an invariant of framed multi-linkoids.*

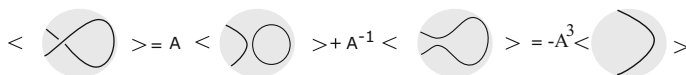


Figure 6. Behavior of the Kauffman bracket polynomial under a R-I move

Proof. The Kauffman bracket polynomial for multi-linkoids behaves the same under Reidemeister moves as for knots and knotoids. Thus, the verification of invariance for multi-linkoids under FR-I, R-II and R-III moves runs similarly with the case of knots. \square

In Fig. 6, we illustrate how $\langle L \rangle$ changes under a R-I move that may take place on a knotoid or a knot component of a multi-linkoid diagram L . It is clear that multiplication of $\langle L \rangle$ by $(-A^3)^{-w(L)}$, where $w(L)$ is the writhe of L , cancels the multiplicative term $-A^3$ resulting from the R-I move.

Definition 2.3. We define the normalized Kauffman bracket polynomial of a multi-linkoid diagram L as

$$\overline{\langle L \rangle}(A^{\pm 1}, \lambda) = (-A^3)^{-w(L)} \langle L \rangle(A^{\pm 1}, \lambda).$$

Proposition 2.4. *The normalized Kauffman bracket polynomial is an invariant of multi-linkoids.*

Proof. It is sufficient to observe that multiplying the Kauffman bracket polynomial of a multi-linkoid diagram L with $(-A^3)^{-w(L)}$ cancels the change of the bracket polynomial under a R-I move. This can be verified as in the case of knotoids [39]. \square

We now introduce an ordered version of the bracket polynomial for ordered multi-linkoids. Let L be an ordered multi-linkoid diagram in S^2 or \mathbb{R}^2 . The endpoints of L are enumerated with respect to the ordering induced by the ordering on the knotoid components of L as discussed in Sect. 1. States of L are obtained as explained above by smoothing all crossings of L with A and B smoothings. Closed components of a state are assigned to $-A^2 - A^{-2}$ and an open component is assigned to the variable λ_{ij} , where $i < j$ are the integer labels at the tail and the head of the component, respectively. We define the ordered bracket polynomial of L as an integer coefficient Laurent polynomial in variables A, A^{-1}, λ_{ij} ($i < j$) as follows.

Definition 2.5. The *ordered bracket polynomial* of an ordered multi-linkoid diagram L , $\langle L \rangle_{\bullet}$ is defined to be the sum

$$\langle L \rangle_{\bullet}(A^{\pm 1}, \{\lambda_{ij}\}_{i < j}) = \sum_{\sigma_i} \langle K \mid \sigma \rangle (-A^2 - A^{-2})^{|\text{c}|} \prod_{\Lambda} \lambda_{ij}, \quad (2)$$

where the sum is taken over all states of L , $\langle K \mid \sigma \rangle$ is the product of the smoothing labels of a state σ_i and Λ is the collection of open components in the state σ_i .

Note that if L is a multi-knotoid diagram, the ordering on L is trivial since there is only one knotoid component of L . Then, the ordered bracket

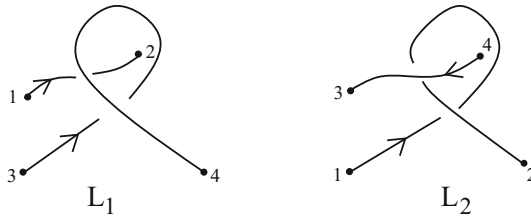


Figure 7. Two ordered linkoids that are distinguished by the ordered bracket polynomial

polynomial of L can be assumed to be equal to the Kauffman bracket polynomial of L with $\lambda_{12} = \lambda = 1$.

Proposition 2.6. *The ordered bracket polynomial turns into an invariant of ordered multi-linkoids when multiplied with $(-A^3)^{-w}$.*

Proof. It is clear that R-0, R-II, and R-III moves preserve the ordering on the knotoid components of a multi-linkoid diagram, and the invariance of the polynomial under these moves follows similarly as the invariance of the bracket polynomial. A R-I move changes the ordered bracket polynomial by $(-A)^{\pm 3}$ as in the case of the bracket polynomial so that multiplying the ordered bracket polynomial with $(-A^3)^{-w}$ makes it invariant under R-I moves as well. \square

Example 1. In Fig. 7, two ordered linkoid diagrams with two components are given. Explicit computation shows that the normalized Kauffman bracket polynomial of these linkoids coincide, but they can be distinguished by the normalized ordered bracket polynomial. Precisely, we find

$$\begin{aligned} \langle L_1 \rangle_{\bullet} &= (A^2 + 1)\lambda_{12}\lambda_{34} + \lambda_{13}\lambda_{24} + A^{-2}\lambda_{14}\lambda_{23} \quad \text{and} \\ \langle L_2 \rangle_{\bullet} &= (A^2 + 1)\lambda_{12}\lambda_{34} + \lambda_{14}\lambda_{23} + A^{-2}\lambda_{13}\lambda_{24}. \end{aligned}$$

Example 2. In Fig. 8, the linkoid diagrams differ only for the orderings on components. The normalized bracket polynomial is not able to distinguish them. Direct computation of the normalized ordered bracket polynomials shows that the linkoids represent different ordered linkoids. Precisely, we find

$$\begin{aligned} \langle L'_1 \rangle_{\bullet} &= A^3\lambda_{15}\lambda_{23}\lambda_{46} + A(\lambda_{15}\lambda_{24}\lambda_{36} + \lambda_{14}\lambda_{23}\lambda_{56} + \lambda_{16}\lambda_{23}\lambda_{45}) \\ &\quad + A^{-1}(\lambda_{13}\lambda_{24}\lambda_{56} + \lambda_{14}\lambda_{23}\lambda_{56} + \lambda_{16}\lambda_{24}\lambda_{35}) + A^{-3}\lambda_{13}\lambda_{24}\lambda_{56} \quad \text{and} \\ \langle L'_2 \rangle_{\bullet} &= A^3\lambda_{14}\lambda_{26}\lambda_{35} + A(\lambda_{16}\lambda_{24}\lambda_{35} + \lambda_{14}\lambda_{23}\lambda_{56} + \lambda_{14}\lambda_{25}\lambda_{36}) \\ &\quad + A^{-1}(\lambda_{13}\lambda_{24}\lambda_{56} + \lambda_{14}\lambda_{23}\lambda_{56} + \lambda_{15}\lambda_{24}\lambda_{36}) + A^{-3}\lambda_{13}\lambda_{24}\lambda_{56}. \end{aligned}$$

We observe that $\langle L'_1 \rangle_{\bullet} \neq \langle L'_2 \rangle_{\bullet}$ and the normalized ordered bracket polynomials do not coincide.

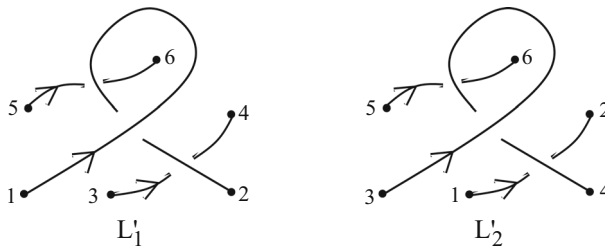


Figure 8. Two ordered linkoids that are distinguished by the ordered bracket polynomial

2.1. The Kauffman Bracket Skein Module

Observe that in the bracket polynomial formulas (1) and (2), we only consider the number of closed components $||c||$ in each state, where each component is assigned the term $-A^2 - A^{-2}$. We can extend the bracket polynomial so that in each state we also keep information about the homology classes of the closed components in c in the complement $S^2 \setminus l$. We do this by introducing the Kauffman bracket skein module (KBSM) of multi-linkoids. Furthermore, we extend this invariant to multi-linkoids in any closed, connected, orientable genus g surface.

Skein modules were independently introduced by Turaev [38] and Przytycki [33], they can be viewed as generalizations of invariants based on the skein relation for knots in 3-manifolds. The idea behind our construction (which is closely related to the original construction) is that we first construct a space of all possible linear combinations of multi-linkoids and in this space impose the relations

$$\begin{aligned} \left[\begin{array}{c} \diagdown \\ \diagup \end{array} \right] &= A \left[\begin{array}{c}) \\ (\end{array} \right] - A^{-1} \left[\begin{array}{c} \smile \\ \frown \end{array} \right], \\ \left[\bigcirc \right] &= (A^2 - A^{-2}) \left[\bullet \right], \end{aligned}$$

which characterize the bracket polynomials given by formulas (1) and (2). For similar constructions see [7, 8, 10, 11, 32].

Definition 2.7. Let Σ be a connected orientable surface of genus g . Let R be a commutative ring with an invertible element A (e.g. the ring of Laurent polynomials $\mathbb{Z}[A, A^{-1}]$) and let $\mathcal{L}_{\Sigma,n}^{\text{fr}}$ be the set of framed multi-linkoids on Σ with $2n$ endpoints. Denote by $R[\mathcal{L}_{\Sigma,n}^{\text{fr}}]$ the free R -module spanned by $\mathcal{L}_{\Sigma,n}^{\text{fr}}$ and by $\mathcal{S}(\mathcal{L}_{\Sigma,n}^{\text{fr}}, R, A)$ the submodule of $R[\mathcal{L}_{\Sigma,n}^{\text{fr}}]$ generated by the following two expressions (relators):

$$\left[\begin{array}{c} \diagdown \\ \diagup \end{array} \right] - A \left[\begin{array}{c}) \\ (\end{array} \right] - A^{-1} \left[\begin{array}{c} \smile \\ \frown \end{array} \right], \tag{3a}$$

$$\left[\bigcirc \right] - (A^2 - A^{-2}) \left[\bullet \right], \tag{3b}$$

where $\left[\begin{array}{c} \diagdown \\ \diagup \end{array} \right]$, $\left[\begin{array}{c}) \\ (\end{array} \right]$, $\left[\begin{array}{c} \smile \\ \frown \end{array} \right]$, $\left[\bigcirc \right]$, and $\left[\bullet \right]$ represent classes of multi-linkoids that are everywhere the same except inside a small disk where they look like the figures indicated.

The Kauffman bracket skein module of multi-linkoids in Σ with $2n$ endpoints is the quotient module

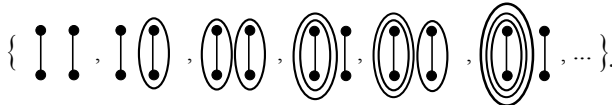
$$\mathcal{K}_{\Sigma,n}^{\text{fr}}(R, A) = R[\mathcal{L}_{\Sigma,n}^{\text{fr}}] / \mathcal{S}(\mathcal{L}_{\Sigma,n}^{\text{fr}}; R, A),$$

i.e. all formal finite linear sums of multi-linkoids in which we enforce the two relations obtained by the expressions (3).

Theorem 2.8. *Let $\mathcal{B}_{\Sigma,n}^{\text{fr}}$ be the set of all framed multi-linkoids in Σ with $2n$ endpoints without crossings and without trivial contractible components in Σ . The module $\mathcal{K}_{\Sigma,n}^{\text{fr}}(R, A)$ is freely generated by $\mathcal{B}_{\Sigma,n}^{\text{fr}}$, i.e. $\mathcal{K}_{\Sigma,n}^{\text{fr}}(R, A) = R[\mathcal{B}_{\Sigma,n}^{\text{fr}}]$.*

In particular,

- (i) $\mathcal{K}_{S^2,1}^{\text{fr}}$ is freely generated by the trivial knotoid \downarrow ,
- (ii) $\mathcal{K}_{\mathbb{R}^2,1}^{\text{fr}}$ is generated by the infinite set $\{\downarrow, \bigcirc\downarrow, \bigcirc\bigcirc\downarrow, \dots\}$,
- (iii) $\mathcal{K}_{\mathbb{R}^2,2}^{\text{fr}}$ is generated by the infinite set



- (iv) $\mathcal{K}_{T^2,1}^{\text{fr}}$ is generated by the infinite set



Proof. In order to prove the theorem, it is enough to show that $\mathcal{B}_{\Sigma,n}^{\text{fr}}$ generates $\mathcal{K}_{\Sigma,n}^{\text{fr}}(R, A)$ and that for a given multi-linkoid $L \in \mathcal{L}_{\Sigma,n}^{\text{fr}}$ the expression $[L] \in \mathcal{K}_{\Sigma,n}^{\text{fr}}(R, A)$, written in terms of the elements in $\mathcal{B}_{\Sigma,n}^{\text{fr}}$, is unique.

For a given representative L of $[L] \in \mathcal{K}_{\Sigma,n}^{\text{fr}}(R, A)$, we can first remove all crossings using (3a) and then remove all trivial components using (3b), we end up with a formal linear sum of elements $\mathcal{B}_{\Sigma,n}^{\text{fr}}$. Elements $\mathcal{B}_{\Sigma,n}^{\text{fr}}$ thus generate the module.

To show that the expression $[L]$, written in terms of elements in $\mathcal{B}_{\Sigma,n}^{\text{fr}}$, is unique, we need to show that it does not depend on any choice we can make during the computation of $[L]$ and that it is invariant under Reidemeister moves for framed linkoid diagrams. We enumerate the crossings of L by ordinals $1, 2, \dots, k$. We first show that the coefficients do not depend on the order we perform crossing eliminations via (3a).

Let $\begin{array}{c} \overset{i}{\diagdown} \\ \overset{j}{\diagup} \\ \diagdown \\ \diagup \end{array}$ represent a multi-linkoid with crossings i and j marked. The coefficients do not depend on the order of crossings smoothings:

$$\begin{array}{c} \overset{i}{\diagdown} \\ \overset{j}{\diagup} \\ \diagdown \\ \diagup \end{array} = A \begin{array}{c}) \\ (\\ \diagdown \\ \diagup \end{array} + A^{-1} \begin{array}{c} \smile \\ \frown \\ \diagdown \\ \diagup \end{array} = A^2 \begin{array}{c}) \\ (\\) \\ (\end{array} + \begin{array}{c}) \\ (\\ \smile \\ \frown \end{array} + \begin{array}{c} \smile \\ \frown \\) \\ (\end{array}$$

$$\begin{aligned}
 & +A^{-2} \overbrace{\underbrace{\quad}^i} \overbrace{\underbrace{\quad}^j} , \\
 \overbrace{\underbrace{\quad}^i} \overbrace{\underbrace{\quad}^j} & = A \overbrace{\underbrace{\quad}^i} \overbrace{\underbrace{\quad}^j} + A^{-1} \overbrace{\underbrace{\quad}^i} \overbrace{\underbrace{\quad}^j} = A^2 \overbrace{\underbrace{\quad}^i} \overbrace{\underbrace{\quad}^j} + \overbrace{\underbrace{\quad}^i} \overbrace{\underbrace{\quad}^j} + \overbrace{\underbrace{\quad}^i} \overbrace{\underbrace{\quad}^j} \\
 & +A^{-2} \overbrace{\underbrace{\quad}^i} \overbrace{\underbrace{\quad}^j} .
 \end{aligned}$$

In addition, the coefficients do not depend on the elimination order of trivial components using the framing relation (3b). Also, it does not depend on the elimination order when a choice is to be made if a crossing or a trivial component is to be eliminated.

Proving the invariance is similar to the case of classical knots. The expression is invariant under Reidemeister move R-II:

$$\begin{aligned}
 \overbrace{\underbrace{\quad}^i} & = A \overbrace{\underbrace{\quad}^i} + A^{-1} \overbrace{\underbrace{\quad}^i} = A^2 \overbrace{\underbrace{\quad}^i} + \overbrace{\underbrace{\quad}^i} + \overbrace{\underbrace{\quad}^i} \\
 & +A^{-2} \overbrace{\underbrace{\quad}^i} = \overbrace{\underbrace{\quad}^i} \overbrace{\underbrace{\quad}^i} ,
 \end{aligned}$$

where we used the framing relation (3b) in the last equality. The expression is also invariant under Reidemeister move R-III:

$$\overbrace{\underbrace{\quad}^i} \overbrace{\underbrace{\quad}^j} = A \overbrace{\underbrace{\quad}^i} \overbrace{\underbrace{\quad}^j} + A^{-1} \overbrace{\underbrace{\quad}^i} \overbrace{\underbrace{\quad}^j} = A \overbrace{\underbrace{\quad}^i} \overbrace{\underbrace{\quad}^j} + A^{-1} \overbrace{\underbrace{\quad}^i} \overbrace{\underbrace{\quad}^j} = \overbrace{\underbrace{\quad}^i} \overbrace{\underbrace{\quad}^j} ,$$

where the second equality holds by invariance under R-II. □

Let L be a multi-linkoid in Σ with $2n$ endpoints. We denote by $[L]_{\mathcal{B}_{\Sigma,n}^{\text{fr}}}$ the class of L in $\mathcal{K}_{\Sigma,n}^{\text{fr}}$ written in terms of elements in the basis $\mathcal{B}_{\Sigma,n}^{\text{fr}}$ (or just $[L]$ if we fix the basis and the ambient space is known from context). Due to Theorem 2.8, $[L]$ is an invariant of unordered framed multi-linkoids.

As in the classical case, we can obtain an invariant of non-framed linkoids by multiplying it by $(-A^3)^{-w(L)}$. The expression

$$\overline{[L]}_{\mathcal{B}_{\Sigma,n}^{\text{fr}}} = (-A^3)^{-w(L)} [L]_{\mathcal{B}_{\Sigma,n}^{\text{fr}}}$$

is an invariant of multi-linkoids in Σ .

Let us now consider the ordered case. For this, we will need the set of multi-linkoids with arbitrary ordering on the vertices (not necessarily consecutive on the endpoints on the same component). More precisely, each endpoint of a multi-linkoid diagram is assigned to exactly one value in $\{1, 2, \dots, 2n\}$. We call the resulting diagram a *vertex-ordered multi-linkoid diagram*.

Definition 2.9. Two vertex-ordered multi-linkoid diagrams are equivalent if there is a finite sequence of Reidemeister moves R-0, R-I, R-II, and R-III that takes one diagram to the other, such that the orderings on vertices of the two diagrams coincide. The equivalent classes are called *vertex-ordered multi-linkoids*.

Definition 2.10. A framed multi-linkoid diagram with an arbitrary ordering on its vertices is called a *framed vertex-ordered multi-linkoid diagram*. *Framed*

vertex-ordered multi-linkoids are equivalent classes given by framed Reidemeister moves.

Definition 2.11. Let $\hat{\mathcal{L}}_{\Sigma,n}^{\text{fr}}$ be the set of all vertex-ordered multi-linkoids with n open components and $\mathcal{S}(\hat{\mathcal{L}}_{\Sigma,n}^{\text{fr}}; R, A)$ be the submodule of the free R -module $R[\hat{\mathcal{L}}_{\Sigma,n}^{\text{fr}}]$ generated by the relators (3). The quotient module

$$\hat{\mathcal{K}}_{\Sigma,n}^{\text{fr}}(R, A) = R[\hat{\mathcal{L}}_{\Sigma,n}^{\text{fr}}] / \mathcal{S}(\hat{\mathcal{L}}_{\Sigma,n}^{\text{fr}}; R, A)$$

is the *Kauffman bracket skein module of vertex-ordered multi-linkoids in Σ with $2n$ endpoints*. As ordered multi-linkoids are just special cases of vertex-ordered multi-linkoids, we will obtain an ordered multi-linkoids invariant through $\hat{\mathcal{K}}_{\Sigma,n}^{\text{fr}}(R, A)$.

Theorem 2.12. Let $\hat{\mathcal{B}}_{\Sigma,n}^{\text{fr}}$ the set of all isotopy classes on Σ of vertex-ordered multi-linkoids on Σ with $2n$ endpoints without crossings and without trivial contractible components. The module $\hat{\mathcal{K}}_{\Sigma,n}^{\text{fr}}(R, A)$ is freely generated by the basis $\hat{\mathcal{B}}_{\Sigma,n}^{\text{fr}}$, i.e. $\hat{\mathcal{K}}_{\Sigma,n}^{\text{fr}}(R, A) = R[\hat{\mathcal{B}}_{\Sigma,n}^{\text{fr}}]$.

Proof. The ordered vertices of vertex-ordered linkoid diagrams lie outside the areas of relations (3). Since the skein module is defined by relations (3), the proof is essentially the same to that of Theorem 2.8. Using operations (3), we can remove all crossings and trivial components, and thus represent every class of a link as a formal sum of elements in $L \in \hat{\mathcal{L}}_{\Sigma,n}^{\text{fr}}$. Clearly, as before, the result also does not depend on the order we perform the operations. To show invariance under Reidemeister moves, we repeat the argument from the proof of Theorem 2.8 verbatim. \square

Remark 2.13. Note that both $\mathcal{B}_{\Sigma,n}^{\text{fr}}$ and $\hat{\mathcal{B}}_{\Sigma,n}^{\text{fr}}$ are sets consisting of isotopy classes of links. The surjective map $\phi : \hat{\mathcal{L}}_{\Sigma,n}^{\text{fr}} \rightarrow \mathcal{L}_{\Sigma,n}^{\text{fr}}$, obtained by removing the enumeration on the vertices, linearly extends to a map $\hat{\mathcal{K}}_{\Sigma,n}^{\text{fr}}(R, A) \rightarrow \mathcal{K}_{\Sigma,n}^{\text{fr}}(R, A)$, where several all elements in $\hat{\mathcal{B}}_{\Sigma,n}^{\text{fr}}$ that differ only by a permutation on their vertices, are mapped to the same element in $\mathcal{B}_{\Sigma,n}^{\text{fr}}$. In fact, $\mathcal{K}_{\Sigma,n}^{\text{fr}}(R, A)$ can be viewed as an orbit space of a group action on $\hat{\mathcal{K}}_{\Sigma,n}^{\text{fr}}(R, A)$. See Examples 3 and 4.

As before, the normalized expression

$$\overline{[L]}_{\hat{\mathcal{B}}_{\Sigma,n}^{\text{fr}}} = (-A^3)^{-w(L)} [L]_{\hat{\mathcal{B}}_{\Sigma,n}^{\text{fr}}}$$

is an invariant of vertex-ordered multi-linkoids on Σ and, as a special case, an invariant of ordered multi-linkoids on Σ .

The following propositions follow directly from construction.

Proposition 2.14. Given an (unordered) multi-linkoid diagram L in S^2 (or \mathbb{R}^2), the Kauffman bracket polynomial of L , $\langle L \rangle (A^{\pm 1}, \lambda)$, is obtained from $[L]$ by replacing each open component with λ and each closed component with $(-A^2 - A^{-2})$.

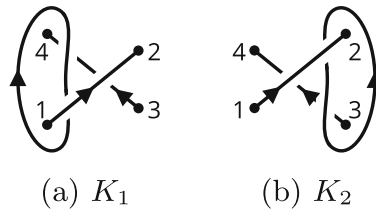


Figure 9. Two oriented multi-knotoids on \mathbb{R}^2

Proposition 2.15. *Given an ordered multi-linkoid L in S^2 (or \mathbb{R}^2), the ordered Kauffman bracket polynomial of L , $\langle L \rangle_\bullet (A^{\pm 1}, \{\lambda_{ij}\}_{(i,j) \in \mathcal{I}})$, where $\mathcal{I} \subset \mathbb{N}^2$ is the index set, is obtained from $\overline{[L]}$ by replacing each open component with endpoints, enumerated by i and j , with λ_{ij} and each closed component with $(-A^2 - A^{-2})$.*

Example 3. Consider the two oriented multi-linkoids K_1 and K_2 in \mathbb{R}^2 in Fig. 9. We have $w(K_1) = w(K_2) = -1$. A straightforward computation shows us

$$\begin{aligned} \overline{[K_1]}_{\mathcal{B}_{\mathbb{R}^2,1}} &= -2A^2 \begin{array}{c} \uparrow^2 \\ \downarrow^4 \end{array} - 2A^4 \begin{array}{c} \uparrow^4 \\ \downarrow^3 \end{array} - A^6 \begin{array}{c} \circlearrowleft \\ \uparrow^3 \\ \downarrow^4 \end{array}, \\ \overline{[K_2]}_{\mathcal{B}_{\mathbb{R}^2,1}} &= -2A^2 \begin{array}{c} \uparrow^2 \\ \downarrow^4 \end{array} - 2A^4 \begin{array}{c} \uparrow^4 \\ \downarrow^3 \end{array} - A^6 \begin{array}{c} \circlearrowright \\ \uparrow^4 \\ \downarrow^3 \end{array}, \end{aligned} \tag{4}$$

By Proposition 2.15, we can obtain the Kauffman bracket polynomial from the Kauffman bracket skein modules by the replacements

$$\begin{aligned} \begin{array}{c} \uparrow^2 \\ \downarrow^4 \end{array} &\rightarrow \lambda_{12}\lambda_{34}, & \begin{array}{c} \uparrow^4 \\ \downarrow^3 \end{array} &\rightarrow \lambda_{14}\lambda_{23}, \\ \begin{array}{c} \circlearrowleft \\ \uparrow^3 \\ \downarrow^4 \end{array} &\rightarrow (-A^2 - A^{-2})\lambda_{14}\lambda_{23}, & \begin{array}{c} \circlearrowright \\ \uparrow^4 \\ \downarrow^3 \end{array} &\rightarrow (-A^2 - A^{-2})\lambda_{14}\lambda_{23}. \end{aligned}$$

The normalized ordered Kauffman bracket polynomial does not distinguish the two multi-linkoids. In fact, we have

$$\langle \overline{K_1} \rangle_\bullet = \langle \overline{K_2} \rangle_\bullet = -2A^2\lambda_{12}\lambda_{34} + (A^8 - A^4)\lambda_{14}\lambda_{23}.$$

Observe that if we consider that the two multi-linkoids lie in S^2 , K_1 and K_2 are isotopic and

$$\overline{[K_1]}_{\mathcal{B}_{S^2,1}} = \overline{[K_1]}_{\mathcal{B}_{S^2,1}} = -2A^2 \begin{array}{c} \uparrow^2 \\ \downarrow^4 \end{array} - 2A^4 \begin{array}{c} \uparrow^4 \\ \downarrow^3 \end{array} - A^6 \begin{array}{c} \circlearrowleft \\ \uparrow^4 \\ \downarrow^3 \end{array}.$$

Example 4. Let us denote by K'_1 and K'_2 two multi-linkoids on \mathbb{R}^2 that are obtained respectively from K_1 and K_2 from Fig. 9, except that we remove information about the orientation and the ordering of the vertices, i.e. if we take the map ϕ from Remark 2.13, it holds $\phi(K_1) = K'_1$ and $\phi(K_2) = K'_2$.

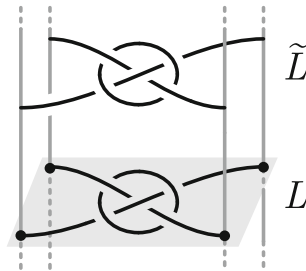


Figure 10. A multi-linkoid diagram L in a plane and the corresponding space curve \tilde{L} with endpoints on the lines perpendicular to the plane

Since it also holds that

$$\phi(\mathbb{I}_1^2 \mathbb{I}_3^4) = \phi(\mathbb{I}_1^4 \mathbb{I}_2^3) = \mathbb{I} \mathbb{I} \quad \text{and} \quad \phi(\mathbb{I}_1^4 \mathbb{I}_2^3) = \phi(\mathbb{I}_1^4 \mathbb{I}_2^3) = \mathbb{I} \mathbb{I},$$

it follows from (4) that

$$\overline{[K'_1]}_{\mathcal{B}_{\mathbb{R}^2,1}} = \overline{[K'_2]}_{\mathcal{B}_{\mathbb{R}^2,1}} = -2(A^2 + A^4) \mathbb{I} \mathbb{I} - A^6 \mathbb{I} \mathbb{I},$$

which we could also compute easily from the definition.

3. Spatial Graphs and Multi-linkoids

Knotoids in \mathbb{R}^2 and S^2 can be described geometrically via open space curves whose endpoints are attached to two parallel lines or a class of spatial graphs called Θ -graphs, respectively, as described in [39] and [14]. This geometric approach can directly be extended to multi-linkoids in \mathbb{R}^2 , so that they can be understood as unions of space curves whose endpoints are attached to a number of parallel lines perpendicular to the plane of the diagram, see Fig. 10.

In the sequel, we discuss a geometric interpretation of multi-linkoids in S^2 by introducing generalized Θ -graphs.

Definition 3.1. A *spatial graph* Γ in S^3 (or \mathbb{R}^3) of a graph G is an embedding $\Gamma : G \hookrightarrow S^3$ (or \mathbb{R}^3).

Definition 3.2. Two spatial graphs are *equivalent* if they are ambient isotopic.

Definition 3.3. A *regular projection* $p(\Gamma)$ of a spatial graph Γ is an orthogonal projection of Γ to a plane in \mathbb{R}^3 (or a sphere in S^3) that is locally one-to-one and the inverse image of every point y in $p(\Gamma)$ contains either one or two points, if $p^{-1}(\Gamma)$ contains two points, neither of these points is a vertex.

Definition 3.4. A *spatial graph diagram* is a regular projection of a spatial graph to \mathbb{R}^2 in \mathbb{R}^3 (or S^2 in S^3), endowed with under or over information at each intersection of the edges.

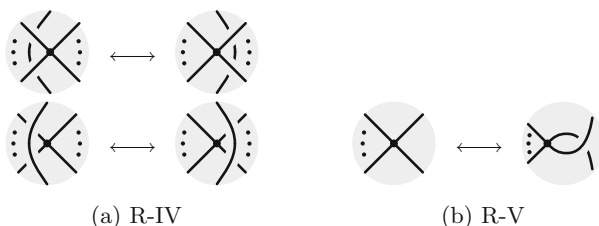


Figure 11. Reidemeister moves for spatial graph diagrams involving a vertex. The vertex involved in the move can be of any degree

The following theorem is an analog of Reidemeister’s theorem, which makes it possible to study spatial graphs through their diagrams.

Theorem 3.5 (Kauffman [21]). *Two spatial graphs diagrams represent ambient isotopic spatial graphs if and only if one of them can be transformed into the other by a finite sequence of move R-0, R-I, R-II, R-III involving the edges (Fig. 2) and moves R-IV and R-V involving the vertices (Fig. 11).*

Definition 3.6. A Θ -graph is a spatial graph with two labeled vertices v_0, v_1 and three labeled edges e_+, e_0, e_- connecting the vertices. Two Θ -graphs are *equivalent* if there is an orientation preserving isotopy of S^3 taking one to another that preserves the labeling of the vertices and the edges.

Definition 3.7. A Θ -graph is called *simple* if the edges e_+ and e_- bound a 2-disk in \mathbb{R}^3 .

As described in [39], a knotoid diagram in S^2 can be uniquely associated with a simple Θ -graph by assuming the two vertices of the graph as the endpoints of the knotoid diagram and the e_0 edge as the knotoid diagram itself. The edge e_+ is unknotted and goes above the rest of the diagram and the edge e_- is unknotted and goes below the rest of the diagram.

Theorem 3.8 ([39]). *There is a bijective map between the set of all isotopy classes of knotoids in S^2 and the set of all simple Θ -graphs.*

We now generalize this correspondence to multi-linkoids by introducing generalized Θ -graphs and then extract invariants for multi-linkoids from spatial graph invariants.

Definition 3.9. A *generalized Θ -graph* is a connected graph embedded in S^3 with an even number, say $2n, n \in \mathbb{N}$, of trivalent vertices, labeled v_i and w_i where $i \in \{1, \dots, n\}$, and exactly two vertices $v_\infty, v_{-\infty}$ that are located at $N(0, 0, 0, 1) \in S^3$ and $S(0, 0, 0, -1) \in S^3$, respectively. The edge set $E(G)$ consists of edges $\{v_i w_i\}_{i=1}^n$, edges $\{v_i v_\infty\}_{i=1}^n$ and edges $\{v_i v_{-\infty}\}_{i=1}^n$ connecting v_i and the vertices v_∞ and $v_{-\infty}$, and edges $\{w_i v_\infty\}_{i=1}^n$ and $\{w_i v_{-\infty}\}_{i=1}^n$ connecting w_i and the points v_∞ and $v_{-\infty}$. Note that each vertex of a pair (v_i, w_i) is adjacent to both v_∞ and $v_{-\infty}$.

Definition 3.10. A generalized Θ -graph is simple if for every pair of vertices in $E = \{v_1, \dots, v_n, w_1, \dots, w_n\}$, the subgraph induced by the edges connecting the pair of vertices to v_∞ and $v_{-\infty}$ bounds a disk. See the right hand side of Fig. 12 as an example.

Definition 3.11. Consider $S^3 = \mathbb{R}^3 \cup \{\infty\}$. A simple generalized Θ -graph in S^3 is *standard* if

- (i) the vertices that are labeled by v_i, w_j lie on $\mathbb{R}^2 \times \{0\} \subset \mathbb{R}^3$ at different horizontal positions for all $i, j \in \{1, \dots, n\}, i \neq j$,
- (ii) for all i , where $i \in \{1, \dots, n\}$, the edges $v_i v_\infty$ and $w_i v_\infty$ lie in the upper half-space while the edges $v_i v_{-\infty}$ and $w_i v_{-\infty}$ lie in the lower half-space,
- (iii) there is no braiding between the edges $v_i v_{\pm\infty}$ and $v_j v_{\pm\infty}$ or $w_i v_{\pm\infty}$ and $w_j v_{\pm\infty}$.

Given a generalized simple Θ -graph, we can always move (using isotopy) the vertices $E = \{v_1, \dots, v_n, w_1, \dots, w_n\}$ in the plane $\mathbb{R}^2 \times \{0\} \subset \mathbb{R}^3$ in such a way, that condition (i) is satisfied. In addition, we can move the points v_∞ and $v_{-\infty}$ by isotopy, respectively, to the upper and lower half-space. Since any two vertices $u, u' \in E$, together with the vertices v_∞ and $v_{-\infty}$, bound a disk, the edges connecting v_∞ and $v_{-\infty}$ can be moved by isotopy so that (ii) and (iii) are also satisfied. Thus, the following proposition holds (Fig. 12):

Proposition 3.12. *Every simple generalized Θ -graph is equivalent to a standard generalized Θ -graph.*

Let L be a linkoid diagram in S^2 with $2n$ endpoints. We assign to L a standard generalized Θ -graph embedded in S^3 , which we denote by $\Theta(L)$. The graph $\Theta(L)$ is constructed as follows. We label each component of L by $i \in \{1, \dots, n\}$, and denote by v_i the tail and by w_i and the head of component i , such that component i corresponds to an edge $v_i w_i$ in $\Theta(L)$. We also add two vertices, denoted by v_∞ and $v_{-\infty}$ at $N(0, 0, 0, 1) \in S^3$ and $S(0, 0, 0, -1) \in S^3$, respectively.

Then we add edges $v_i v_\infty, v_i v_{-\infty}, w_i v_\infty,$ and $w_i v_{-\infty}$ that connect the vertices v_i and w_i for all $i \in \{1, \dots, 2n\}$ to the vertices v_∞ and $v_{-\infty}$ in a way that the edges $v_i v_\infty$ and $w_i v_\infty$ lie in the upper hemisphere while the edges $v_i v_{-\infty}$ and $w_i v_{-\infty}$ lie in the lower hemisphere of S^3 . Moreover, every quadruplet of edges $v_i v_\infty, v_i v_{-\infty}, w_j v_\infty,$ and $w_j v_{-\infty}$ bounds a disk. The resulting graph, denoted by $\Theta(L)$ is a simple generalized Θ -graph with $2n + 2$ vertices such that $2n$ vertices are of degree 3, and the two vertices at the poles are of degree $2n$.

Theorem 3.13. *There is a bijective map between the set of all linkoids in S^2 , $\mathcal{L}(S^2)$ and the set of all simple generalized Θ -graphs in S^3 , $\Theta(S^3)$.*

Proof. Let $\theta : \mathcal{L}(S^2) \rightarrow \Theta(S^3)$ be defined as $\theta(L) = \Theta(L)$, where $L \in \mathcal{L}(S^2)$ and $\Theta(L) \in \Theta(S^3)$ is the simple generalized spatial graph assigned to L as described above.

To prove the statement, we show that the map θ is a bijection. For this, we first show that θ is well-defined. That is, we show that if two linkoid

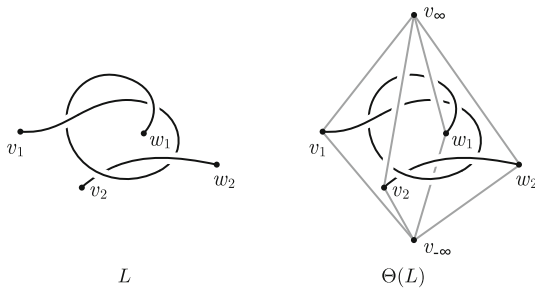


Figure 12. A linkoid and the corresponding generalized Θ -graph

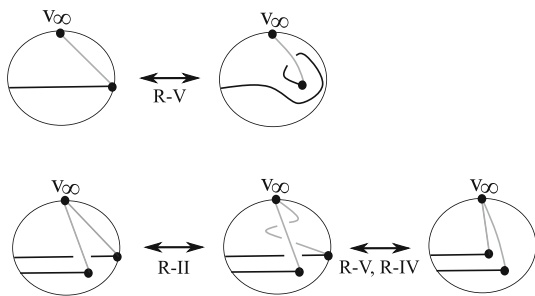


Figure 13. Spatial graph moves involving vertices. Planar isotopy of the knotoid (in bold) can be expressed with a sequence of Reidemeister moves of the corresponding θ -graph diagram (bold and non-bold edges)

diagrams are equivalent, then the assigned simple generalized Θ -graph diagrams are equivalent. By definition, Reidemeister moves of linkoid diagrams take place away from the endpoints. We observe that each Reidemeister move on a linkoid diagram L transforms to the corresponding Reidemeister move on a diagram of $\Theta(L)$, if the move does not interact with any of the edges connecting the vertices v_i, w_j to the vertices $v_{\pm\infty}$ in $\Theta(L)$. If the move interacts with any of the edges connecting v_i, w_j to $v_{\pm\infty}$ in $\Theta(L)$, then the Reidemeister move that takes place on the linkoid diagram transforms to a combination of Reidemeister moves of the diagram of $\Theta(L)$.

Isotopy of S^2 (R-0 moves) may displace endpoints of the linkoid diagram and in this case it transforms to a combination of spatial graph Reidemeister moves including R-IV and R-V-moves on the corresponding generalized θ -graph diagram. See Fig. 13 for two of the related instances.

We show now that the map θ has an inverse so that there is a unique linkoid assigned to each simple generalized Θ -graph. This would prove the map θ is a bijection.

Let θ be a simple generalized Θ -graph. By Proposition 3.12, we can consider θ standard so that the vertices v_i, w_i lie in a plane for all $i \in \{1, \dots, 2n\}$. For every pair of vertices v_i and w_i , there are two lines passing through the



Figure 14. Local replacements $t(G, v)$ at a vertex v

vertices and are orthogonal to the plane, and these lines span a vertical plane. Let P_i denote this plane, $i \in \{1, \dots, n\}$.

On the other hand, each quadruplet of edges $v_i, v_{\pm\infty}$ and $w_i, v_{\pm\infty}$ bound a disk for all $i \in \{1, \dots, 2n\}$ that can be deformed to a disk so that there are only finitely many intersections with each edge connecting the vertices v_i to w_i , and each disk that is bounded by $v_i, v_{\pm\infty}$ and $w_i, v_{\pm\infty}$ for some i is a subset of the plane P_i spanned by v_i and w_i . Let D_i denote such disk spanned by $v_i, v_{\pm\infty}, w_i, v_{\pm\infty}$, $i \in \{1, \dots, 2n\}$.

We pull pieces of strands of the edge $v_i w_i$ that intersect $P_i - D_i$ across the vertices v_i or w_i so that $v_i w_i$ have intersections only with D_i . Note here that the edge $v_i w_i$ can also intersect $P_j - D_j$ for some $j \neq i$. We pull the intersections of $v_i w_i$ with $P_j - D_j$ across the vertices v_j, w_j .

Then the union of the edges $v_i w_i$ and the vertices $\{v_i, w_i\}$ of the resulting graph forms a linkoid diagram in the plane when the intersections with D_i 's are projected to the plane. In fact, the resulting linkoid diagram differs with respect to the choice of the vertex (v_i or w_i) but considering the resulting linkoid diagram in S^2 provides the equivalence of the diagrams via isotopy of S^2 . □

Theorem 3.13 can be generalized to multi-linkoids directly by considering generalized Θ -graphs with knot components.

4. A Colored Version of Kauffman's T Invariant

In [21] an invariant T of spatial graphs in S^3 was introduced as follows.

Definition 4.1. Let G be a spatial graph (a graph embedded in S^3 or \mathbb{R}^3) and let v be a vertex of G of degree d . We associate to (G, v) a set consisting of $\frac{d(d-1)}{2}$ spatial graphs obtained by connecting two pairs of edges at this vertex and leaving all other edges as free ends (leaves) as in Fig. 14. We call such an operation a *local replacement*.

Let $T(G)$ be the set of all local replacements made on all vertices of G , where, in addition, we remove all non-closed curves. More precisely, let $t(G, v)$ denote the set of spatial graphs obtained by local replacements on the vertex v (as in Fig. 14) and let $c(G)$ be the set of closed circles of a (possibly non-connected) spatial graph G . T is a map from the set of spatial graphs to the set of links defined recursively as

$$T(G) = \begin{cases} \bigcup_{g \in t(G, v)} T(g), & \text{where } v \text{ is a vertex of } G, \\ \{c(G)\}, & \text{if } G \text{ contains no vertices.} \end{cases}$$

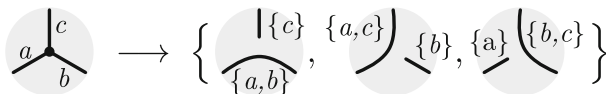


Figure 15. Colored local replacements at a vertex

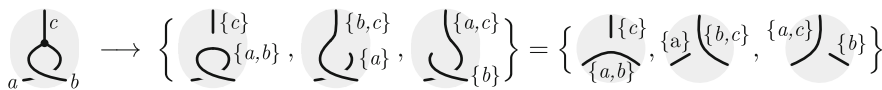


Figure 16. Colored local replacements at a vertex

Note that the invariant T is also known in literature as the *unplugging invariant* [17].

Theorem 4.2 ([21]). *Let G be a spatial graph. Then the collection $T(G)$, taken up to ambient isotopy, is a topological invariant of G .*

We will extend T to an invariant of edge-colored graphs, T_{col} , which we will use as an invariant of generalized Θ -graphs.

Let (G, C) be an edge-colored spatial graph, i.e. a spatial graph G equipped with a coloring function $\gamma : E(G) \rightarrow \Gamma$ for a set of colors Γ . We define a colored local replacement as a local replacement of uncolored graphs, where, in addition, we color the new arcs by a subset $\omega \subseteq \Gamma$, such that ω consists of all the colors of the edges in the preimage of the replacement as in Fig. 15.

Now T_{col} is defined exactly as T , except that the local replacement is replaced by the colored version presented in Fig. 15.

Clearly, the value of $T_{\text{col}}(G)$ is a set of colored links with colors in the power set $\mathcal{P}(C)$. Such sets can be distinguished using any colored link invariant, for example, the multivariate Alexander polynomial [31, 37] or the colored Jones-type polynomial [2].

Theorem 4.3. *Let (G, γ) be an edge-colored spatial graph, the collection of colored links $T_{\text{col}}(G)$, taken up to ambient isotopy, is a topological invariant of (G, γ) .*

Proof. It is easy to check that Reidemeister moves R-I – R-IV do not change the isotopy types of elements in $T_{\text{col}}(G)$ and the move R-V permutes the elements (compare Figs. 15 and 16). \square

Example 5. Consider the Θ -curve Θ_{3_1} from [30], where we color two edges with color 1 and one edge with color 2 as depicted in Fig. 17 (cf. bonded knots independently introduced in [10] and [1]). We have three coloring choices of colored graphs, which we name A , B , and C .

It holds $T_{\text{col}}(A) = T_{\text{col}}(B) \neq T_{\text{col}}(C)$. One can check, using Reidemeister moves, that A and B are ambient isotopic and C is neither ambient isotopic to A nor B , thus T_{col} is able to detect the two isotopy classes.

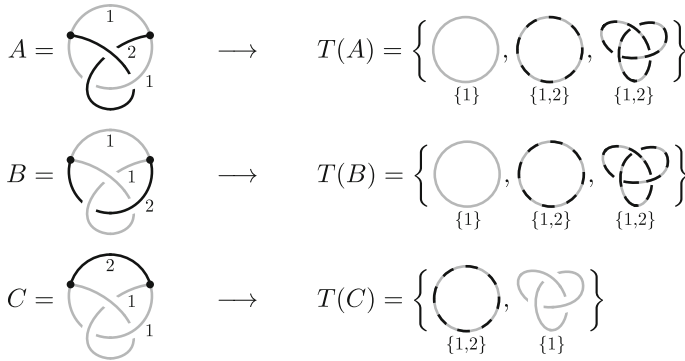


Figure 17. Three 2-colorings of Θ_3_1 and their values under the function T_{col}

Given a multi-linkoid L , we can construct different invariants, based on T_{col} , by modifying the coloring function on $\Theta(L)$. The invariants vary in strength and function:

- An invariant of unordered unoriented multi-linkoids: choose $c(v_i w_i) = 0$ for the edges of K and choose $c(v_i v_{\pm\infty}) = c(w_i v_{\pm\infty}) = 1$ for the edges adjacent to points v_{∞} and $v_{-\infty}$,
- An invariant of unordered unoriented multi-linkoids (stronger version): choose $c(v_i w_i) = 0$ for the edges of K and choose $c(v_i v_{\infty}) = c(w_i v_{\infty}) = 1$ and $c(v_i v_{-\infty}) = c(w_i v_{-\infty}) = -1$,
- An invariant of unordered oriented multi-linkoids: choose $c(v_i w_i) = 0$ for the edges of K and choose $c(v_i v_{\pm\infty}) = 1$ and $c(w_i v_{\pm\infty}) = 2$,
- An invariant of unordered oriented multi-linkoids (stronger version): choose $c(v_i w_i) = 0$ for the edges of K and choose $c(v_i v_{\infty}) = 1, c(v_i v_{-\infty}) = -1, c(w_i v_{\infty}) = 2, c(w_i v_{-\infty}) = -2$,
- An invariant of ordered multi-linkoids: choose $c(v_i w_i) = i$ for the edges of K and choose $c(v_i v_{\pm\infty}) = (i, 1)$ and $c(w_i v_{\pm\infty}) = (i, 2)$,
- An invariant of ordered multi-linkoids (stronger version): choose $c(v_i w_i) = i$ for the edges of K and choose $c(v_i v_{\infty}) = (i, 1), c(w_i v_{\infty}) = (i, 2), c(w_i v_{-\infty}) = (i, -1)$ and $c(w_i v_{-\infty}) = (i, -2)$.

Acknowledgements

Gabrovšek was supported by the Slovenian Research Agency program P1-0292 and grants J1-4031. The authors thank the anonymous referees for their suggestions and comments.

Funding Open access publishing supported by the Slovenian Research Agency and Central Technical Library in Ljubljana.

Data Availability Statement This manuscript has no associate data.

Open Access This article is licensed under a Creative Commons Attribution 4.0 International License, which permits use, sharing, adaptation, distribution and reproduction in any medium or format, as long as you give appropriate credit to the original author(s) and the source, provide a link to the Creative Commons licence, and indicate if changes were made. The images or other third party material in this article are included in the article's Creative Commons licence, unless indicated otherwise in a credit line to the material. If material is not included in the article's Creative Commons licence and your intended use is not permitted by statutory regulation or exceeds the permitted use, you will need to obtain permission directly from the copyright holder. To view a copy of this licence, visit <http://creativecommons.org/licenses/by/4.0/>.

Publisher's Note Springer Nature remains neutral with regard to jurisdictional claims in published maps and institutional affiliations.

References

- [1] Adams, C., Devadoss, J., Elhamdadi, M., Mashaghi, A.: Knot theory for proteins: gauss codes, quandles and bondles. *J. Math. Chem.* **58**(8), 1711–1736 (2020)
- [2] Aicardi, F.: An invariant of colored links via skein relation. *Arnold Math. J.* **2**(2), 159–169 (2016)
- [3] Barbensi, A., Buck, D., Harrington, H.A., Lackenby, M.: Double branched covers of knotoids. (preprint) (2018). [arXiv:1811.09121](https://arxiv.org/abs/1811.09121) [math.GT]
- [4] Barbensi, A., Goundaroulis, D.: f -distance of knotoids and protein structure. *Proc. Roy. Soc. A* **477**(2246) (2021)
- [5] Bartolomew, A.: Knotoids. <http://www.layer8.co.uk/maths/knotoids/index.htm> (2021)
- [6] Diamantis, I.: Knotoids, pseudo knotoids, braidoids and pseudo braidoids on the torus. *Commun. Korean Math. Soc.* **37**(4), 1221–1248 (2022)
- [7] Diamantis, I., Lambropoulou, S.: A new basis for the homflypt skein module of the solid torus. *J. Pure Appl. Algebra* **220**(2), 577–605 (2016)
- [8] Diamantis, I., Lambropoulou, S.: An important step for the computation of the HOMFLYPT skein module of the lens spaces $l(p, 1)$ via braids. *J. Knot Theory Ramificat.* 1940007 (2019)
- [9] Forgan, R.S., Sauvage, J.-P., Stoddart, J.F.: Chemical topology: complex molecular knots, links, and entanglements. *Chem. Rev.* **111**(9), 5434–5464 (2011)
- [10] Gabrovšek, B.: An invariant for colored bonded knots. *Stud. Appl. Math.* **146**(3), 586–604 (2021)
- [11] Gabrovšek, B., Mroczkowski, M.: Link diagrams in Seifert manifolds and applications to skein modules. In: *Springer Proceedings in Mathematics and Statistics* pages 117–141. Springer International Publishing (2017)
- [12] Goundaroulis, D., Dorier, J., Benedetti, F., Stasiak, A.: Studies of global and local entanglements of individual protein chains using the concept of knotoids. *Sci. Rep.* **7**(1) (2017)

- [13] Goundaroulis, D., Gügümcü, N., Lambropoulou, S., Dorier, J., Stasiak, A., Kauffman, L.: Topological models for open-knotted protein chains using the concepts of knotoids and bonded knotoids. *Polymers* **9**(12), 444 (2017)
- [14] Gügümcü, N., Kauffman, L.H.: New invariants of knotoids. *Eur. J. Combin.* **65**, 186–229 (2017)
- [15] Gügümcü, N., Kauffman, L.H.: Quantum invariants of knotoids. *Comm. Math. Phys.* **387**(3), 1681–1728 (2021)
- [16] Gügümcü, N., Kauffman, L.H.: Parity, virtual closure and minimality of knotoids. *J. Knot Theory Ramificat.* **30**(11) (2021)
- [17] Gügümcü, N., Gabrovšek, B., Kauffman, L.H.: Invariants of bonded knotoids and applications to protein folding. *Symmetry* **14**, 8 (2022)
- [18] Gügümcü, N., Lambropoulou, S.: Knotoids, braidoids and applications. *Symmetry* **9**(12), 315 (2017)
- [19] Gügümcü, N., Nelson, S.: Biquandle coloring invariants of knotoids. *J. Knot Theory Ramificat.* **28**(04), 1950029 (2019)
- [20] Gügümcü, N., Nelson, S., Oyamaguchi, N.: Biquandle brackets and knotoids. *J. Knot Theory Ramificat.* **30**(09) (2021)
- [21] Kauffman, L.H.: Invariants of graphs in three-space. *Trans. Am. Math. Soc.* **311**(2), 697 (1989)
- [22] Kauffman, L.H.: Virtual knot theory. *Eur. J. Combin.* **20**(7), 663–691 (1999)
- [23] Kauffman, L.H.: Introduction to virtual knot theory. *J. Knot Theory Ramificat.* **21**(13), 1240007 (2012)
- [24] Kodokostas, D., Lambropoulou, S.: Rail knotoids. *J. Knot Theory Ramificat.* **28**(13), 1940019 (2019)
- [25] Korablev, P.G., May, Y.K.: Knotoids and knots in the thickened torus. *Sib. Math. J.* **58**(5), 837–844 (2017)
- [26] Kutluay, D.: Winding homology of knotoids (preprint) (2020). [arXiv:2002.07871](https://arxiv.org/abs/2002.07871) [math.GT]
- [27] Liang, C., Mislow, K.: Knots in proteins. *J. Am. Chem. Soc.* **116**(24), 11189–11190 (1994)
- [28] Millett, K.C., Rawdon, E.J., Stasiak, A., Sułkowska, J.I.: Identifying knots in proteins. *Biochem. Soc. Trans.* **41**(2), 533–537 (2013)
- [29] Moltmaker, W.: Framed knotoids and their quantum invariants. *Commun. Math. Phys.* **393**, 1035–1061 (2021)
- [30] Moriuchi, H.: An enumeration of theta-curves with up to seven crossings. *J. Knot Theory Ramificat.* **18**(02), 167–197 (2009)
- [31] Morton, H.R.: The multivariable Alexander polynomial for a closed braid. In: *Low-dimensional Topology* ed. Hanna Nencka, *Contemporary Mathematics* 233, Amer. Math. Soc (1999)
- [32] Mroczkowski, M.: The Dubrovnik and Kauffman skein modules of the lens spaces $l_{p,1}$. *J. Knot Theory Ramificat.* **27**(03), 1840004 (2018)
- [33] Przytycki, J.H.: Skein modules of 3-manifolds. *Bull. Pol. Acad. Sci. Math.* **39**(1–2), 91–100 (1991)
- [34] Siebert, J., Kivel, A., Atkinson, L., Stevens, T., Laue, E., Virnau, P.: Are there knots in chromosomes? *Polymers* **9**(12), 317 (2017)
- [35] Sułkowska, J.I., Sułkowski, P., Szymczak, P., Cieplak, M.: Stabilizing effect of knots on proteins. *Proc. Natl. Acad. Sci.* **105**(50), 19714–19719 (2008)

- [36] Tarkaev, V.: A homological casson type invariant of knotoids. *Results Math.* **76**(3)(2021)
- [37] Torres, G.: On the alexander polynomial. *Ann. Math.* **57**(1), 57 (1953)
- [38] Turaev, V.G.: Conway and kauffman modules of a solid torus. *J. Soviet Math.* **52**(1), 2799–2805 (1990)
- [39] Turaev, V.: Knotoids. *Osaka J. Math.* **49**(1), 195–223 (2012)
- [40] Virnau, P., Mirny, L.A., Kardar, M.: Intricate knots in proteins: function and evolution. *PLOS Comput. Biol.* **2**(9) (2006)

Boštjan Gabrovšek
Faculty of Mechanical Engineering
University of Ljubljana
Aškerčeva 6
1000 Ljubljana
Slovenia
e-mail: bostjan.gabrovsek@fs.uni-lj.si

and

Institute of Mathematics, Physics, and Mechanics
Jadranska ulica 19
1000 Ljubljana
Slovenia

Neslihan Gügümcü
Department of Mathematics
Izmir Institute of Technology
Izmir
Turkey
e-mail: neslihangugumcu@iyte.edu.tr

Received: May 23, 2022.

Revised: February 19, 2023.

Accepted: February 21, 2023.